AIMS Mathematics

https://www.aimspress.com/journal/Math

AIMS Mathematics, 9(11): 32674–32695.
DOI:10.3934/math.20241564
Received: 12 September 2024
Revised: 22 October 2024
Accepted: 08 November 2024
Published: 19 November 2024

Research article

A novel approach is proposed for obtaining exact travelling wave solutions to the space-time fractional Phi-4 equation

Ikram Ullah[1,*], Muhammad Bilal[1], Aditi Sharma[2,*], Hasim Khan[3,*], Shivam Bhardwaj[4] and Sunil Kumar Sharma[5,*]

[1] School of Mathematics and Statistics, Central South University, Changsha 410083, Hunan, China

[2] Department of Computer Science and Engineering, Symbiosis Institute of Technology, Symbiosis International (Deemed University), Pune, India

[3] Department of Mathematics, College of Science, Jazan University, P. O. Box 114, Jazan 45142, Saudi Arabia

[4] Mccombs School of Business, University of Texas at Austin, USA

[5] Department of Information Systems College of Computer and Information Sciences Majmaah University, Majmaah 11952, Saudi Arabia

* **Correspondence:** Email: ikramullah@csu.edu.cn, ikramullahcsu@yahoo.com, aditi.sharma@ieee.org s.sharma@mu.edu.sa, hhanif@jazanu.edu.sa.

Abstract: Complex physical occurrences currently need the use of nonlinear fractional partial differential equations. This paper provides a new approach to using the conformable derivative of Atangana to achieve exact travelling wave solutions to the space time-fractional Phi-4 problem. Our method enables a more profound comprehension of complex mathematical physics processes. We validate the solutions and demonstrate the effectiveness of our approaches in solving difficult nonlinear problems in nuclear and particle physics. Singular solutions can be retrieved by using the proposed method on nonlinear partial differential equations (NFPDEs). Our results are shown using contour and three-dimensional charts, which demonstrate various soliton formations for varying parameter values in the nonlinear zone. This study contributes to our growing knowledge of optical soliton.

Keywords: nonlinear fractional partial differential equations (NFPDEs); the space time-fractional Phi-4 equation; solutions for travelling waves; Atangana's conformable derivative; solutions for solitons; mathematical physics; nuclear physics; particle physics
Mathematics Subject Classification: 65F10, 65H10, 90C30, 90C33

1. Introduction

Recent years have seen an explosion in the study of fractional differential equations, with the goal of improving the accuracy of simulating multiple complex occurrences. The literature contains a variety of definitions for fractional derivatives. The Riemann Liouville-derivative, Caputo derivative, Caputo Fabrizio-derivative, Jumarie's modified Riemann Liouville-derivative, and Atangana Baleanu-derivative are a few examples of derivatives. In many fields, such as physics, control theory, biology, mathematical physics, applied mathematics, optics, and chemistry, fractional partial differential equations (FPDEs) have found extensive use [1–5], and EDAM [6–10]. This work applies Atangana's beta-derivative to solve the fractional Phi-4 problem accurately in two trustworthy ways. The initial integral approach [11,12] and the functional variable method [13,14] were the two different approaches. Various techniques have been used to solve fractional partial differential equations (FPDEs) in specific applications documented in scientific literature [15–21]. The format of this document is as follows: Some basic definitions and features of Atangana's beta-derivative solution are given in the second part. A thorough examination of the functional variable approach and the first integral approach is given in the third part [22–25]. Using particular approaches, the fourth section presents new and accurate solutions to the fractional Phi-4 problem. This article concludes by providing a thorough presentation of all of its results, making it the final section. Therefore, we employ the $mEDAM$ technique in this study to precisely ascertain the travelling wave solutions for the STFPHI-4 equation. The $1/G'$-expansion method has not yet been employed to obtain the answers, despite the Fisher KPP problem having been solved using a number of numerical, approximative, and analytical ways [26].

Researchers employ EDAM, an improved version of mEDAM, to generate single solutions for nonlinear partial differential equations (NFPDEs). This method converts the NFPDE into a NODE by employing a wave transformation. We transform the zero-order differential equations (NODEs) into a set of nonlinear algebraic equations by proposing a solution based on series. Through the utilisation of tools like Maple, it is possible to identify families of solo solutions for this problem by utilising tools like Maple. Soliton waves possess distinct characteristics. Propagating at a consistent velocity and form, they exhibit self-reinforcing properties. This work used mEDAM to examine many families of kink soliton solutions in order to explore the presence of kink soliton phenomena in STP4E.

2. Definition of Atanganas Beta-deravative

Definition 1. Let $h : [0, \infty) \to \mathrm{R}$ be a function. Then, its fractional conformable derivative of h order α is

$$ {}_{0}^{\wedge}D_t^{\alpha}(g)(t) = \lim_{s\to 0} \frac{h(x + sx^{1-\alpha}) - h(x)}{s}. \tag{2.1}$$

Khalil and colleagues established the aforementioned theorem for fractional derivatives [27]. Still, ordinary derivatives and conformable fractional derivatives have certain similarities. For example, the derivative of the product and the quotient of two functions, respectively. Thus, mathematicians, physicists, and engineers are now undertaking several investigations on conformable derivatives [28].
Definition 2. Atangana's beta-deravative is as follows:

$$ {}_{0}^{\wedge}D_t^{\alpha}(g)(t) = \lim_{s\to 0} \frac{g(t + s[t + \frac{1}{\Gamma(\alpha)}]^{1-\alpha}) - g(t)}{s}. \tag{2.2}$$

Atangana's derivative allows us to eliminate certain weak characteristics of the conformable derivative. As an illustration, the derivative of a differentiable function is precisely 0 at the zero points [29]. Simulations utilising the beta derivative provide a more precise representation of real-world situations in applied mathematics and physics. Furthermore, this enables a more accurate evaluation of the physical characteristics of the photographs. Due to the possession of the highest inherent properties among the basic derivatives, Atangana's derivative may be preferred. The beta derivatives of Atangana exhibit various significant characteristics [30] as follows:

Let $h \neq 0$ and g are two functions differentiable with β-order and $\beta \in (0, 1)$. Then,

$$ {}_0^{\Lambda}D_x^{\alpha} ag(x) + bh(x) = {}_0^{\Lambda} D_x^{\alpha} g(x)a + {}_0^{\Lambda} D_x^{\alpha} h(x)b, \tag{2.3} $$

for $a, b \in R$.

For any $d \in R$

$$ {}_0^{\Lambda}D_x^{\alpha} d = 0, \tag{2.4} $$

$$ {}_0^{\Lambda}D_x^{\alpha}[d]g(x)h(x) = h(x)[{}_0^{\Lambda}D_x^{\alpha}] + g(x)[D_x^{\alpha}h(x)], \tag{2.5} $$

$$ {}_0^{\Lambda}D_x^{\alpha}\frac{g(x)}{h(x)} = \frac{h(x)[{}_0^{\Lambda}D_x^{\alpha}g(x)] + g(x)[D_x^{\alpha}h(x)]}{h^2(x)}. \tag{2.6} $$

Using Eq (2.2),

$$ {}_0^{\Lambda}D_x^{\alpha}g(x) = (x + \frac{1}{\Gamma(\alpha)})^{1-\alpha}\frac{dg(x)}{dx}, \tag{2.7} $$

and

$$ \mu = \frac{\gamma}{\alpha}(x + \frac{1}{\Gamma(\alpha)})^{\alpha}, \tag{2.8} $$

where γ is a constant. Finally, we can write the following:

$$ {}_0^{\Lambda}D_x^{\alpha}g(\mu) = \gamma\frac{dg(\mu)}{d\mu}. \tag{2.9} $$

3. Operational procedure of EDAM

The aim of this section is to give a review of the EDAM. Examine the FPDE using the format provided below [31]:

$$ E(w, D_t^{\alpha}w, D_{h_1}^{\beta}w, D_{h_2}^{\gamma}w, wD_{h_1}^{\beta}w, \ldots) = 0, \;\; 0 < \alpha, \beta, \gamma \leq 1, \tag{3.1} $$

where $w = w(t, h_1, h_2, h_3, \ldots, h_n)$. Using the following procedures, (2.6) may be solved.

Step 1: First, the (3.1) is converted into a variable in the form $w(t, h_1, h_2, h_3, \cdots, h_n) = W(\eta)$, where η denotes a function of $t, h_1, h_2, h_3, \cdots, h_n$, and may be represented in a multitude of ways. This change turns (3.1) into a NODE, which has the following structure:

$$ F(W, W', WW', \ldots) = 0. \tag{3.2} $$

The primes in (3.2) present derivatives with regard to η. (3.2) maybe once or more times be integrated.

Step 2: Then, we assume the following closed form solution to (3.2):

$$V(\Omega) = \sum_{l=-M}^{M} s_j(\zeta(\Omega))^j, \tag{3.3}$$

here, s_j represent parameters requiring approximations.

$$\zeta'(\Omega) = \ln(\Xi)(\kappa + \mu\zeta(\Omega) + \upsilon(\zeta(\Omega))^2), \tag{3.4}$$

where κ, μ, υ are constants and $\Xi > 0,\ \Xi \neq 1$.

Step 3: When we investigate for the homogeneous balance between the greatest order derivative in (3.2) and the most dominant nonlinear element, we find a positive integer M, which is stated in (3.3).

Step 4: Then, we investigate (2.7) or the equation that results from integrating (3.2) with (3.3), and lastly, we combine all of the components in $\zeta(\Omega)$ in the same order to get a polynomial in $\zeta(\Omega)$. For all $s_j s$ and other parameters, if the coefficients of the consequent polynomial are set to zero, an algebraic equation system is obtained.

Step 5: Before that, this system of nonlinear algebraic equations can be solved using Maple.

Step 6: (3.3) and its associated solution $\zeta(\Omega)$ from (3.4), in combination with the unknown parameters, are used to get the travelling wave solutions to (3.1). The families of travelling wave solutions that appears below can be produced by utilising the general solution of (2.9).

Family. 1: For $D < 0$ and $\upsilon \neq 0$, then we have

$$\zeta_1(\Omega) = -\frac{\mu}{2\upsilon} + \frac{\sqrt{-D}\tan_\Xi\left(\frac{1}{2}\sqrt{-D}\Omega\right)}{2\upsilon},$$

$$\zeta_2(\Omega) = -\frac{\mu}{2\upsilon} - \frac{\sqrt{-D}\cot_\Xi\left(\frac{1}{2}\sqrt{-D}\Omega\right)}{2\upsilon},$$

$$\zeta_3(\Omega) = -\frac{\mu}{2\upsilon} + \frac{\sqrt{-D}\left(\tan_\Xi\left(\sqrt{-D}\Omega\right) + \sec_\mho\left(\sqrt{-D}\Omega\right)\right)}{2\upsilon},$$

$$\zeta_4(\Omega) = -\frac{\mu}{2\upsilon} - \frac{\sqrt{-D}\left(\cot_\Xi\left(\sqrt{-D}\Omega\right) + \csc_\Xi\left(\sqrt{-D}\Omega\right)\right)}{2\upsilon},$$

and

$$\zeta_5(\Omega) = -\frac{\mu}{2\upsilon} + \frac{\sqrt{-D}\left(\tan_\Xi\left(\frac{1}{4}\sqrt{-D}\Omega\right) - \cot_\Xi\left(\frac{1}{4}\sqrt{-D}\Omega\right)\right)}{4\upsilon}.$$

Family. 2: For $D > 0$ and $\upsilon \neq 0$, then we have

$$\zeta_6(\Omega) = -\frac{\mu}{2\upsilon} - \frac{\sqrt{D}\tanh_\Xi\left(\frac{1}{2}\sqrt{D}\Omega\right)}{2\upsilon},$$

$$\zeta_7(\Omega) = -\frac{\mu}{2\upsilon} - \frac{\sqrt{D}\coth_\Xi\left(\frac{1}{2}\sqrt{D}\Omega\right)}{2\upsilon},$$

$$\zeta_8(\Omega) = -\frac{\mu}{2\upsilon} - \frac{\sqrt{D}\left(\tanh_\Xi\left(\sqrt{\Delta}\Omega\right) + i\mathrm{sech}_\Xi\left(\sqrt{D}\Omega\right)\right)}{2\upsilon},$$

$$\zeta_9(\Omega) = -\frac{\mu}{2\upsilon} - \frac{\sqrt{D}\left(\coth_\Xi\left(\sqrt{\Delta}\Omega\right) + \mathrm{csch}_\Xi\left(\sqrt{D}\Omega\right)\right)}{2\upsilon},$$

and

$$\zeta_{10}(\Omega) = -\frac{\mu}{2\upsilon} - \frac{\sqrt{D}\left(\tanh_\Xi\left(\frac{1}{4}\sqrt{D}\Omega\right) - \coth_\Xi\left(\frac{1}{4}\sqrt{D}\Omega\right)\right)}{4f}.$$

Family. 3: For $\kappa\upsilon > 0$ and $\mu = 0$,

$$\zeta_{11}(\Omega) = \sqrt{\frac{\kappa}{\upsilon}}\tan_\Xi\left(\sqrt{\kappa\upsilon}\Omega\right),$$

$$\zeta_{12}(\Omega) = -\sqrt{\frac{\kappa}{\upsilon}}\cot_\Xi\left(\sqrt{\upsilon}\Omega\right),$$

$$\zeta_{13}(\Omega) = \sqrt{\frac{\kappa}{\upsilon}}\left(\tan_\Xi\left(2\sqrt{\kappa\upsilon}\eta\right) + \sec_\Xi\left(2\sqrt{d\upsilon}\Omega\right)\right),$$

$$\zeta_{14}(\Omega) = -\sqrt{\frac{\kappa}{\upsilon}}\left(\cot_\Xi\left(2\sqrt{\kappa\upsilon}\Omega\right) + \csc_\Xi\left(2\sqrt{\kappa\upsilon}\Omega\right)\right),$$

and

$$\zeta_{15}(\Omega) = \frac{1}{2}\sqrt{\frac{\kappa}{\upsilon}}\left(\tan_\Xi\left(\frac{1}{2}\sqrt{\kappa\upsilon}\Omega\right) - \cot_\Xi\left(\frac{1}{2}\sqrt{\kappa\upsilon}\Omega\right)\right).$$

Family. 4: For $\kappa\upsilon < 0$ and $\mu = 0$, then we have

$$\zeta_{16}(\Omega) = -\sqrt{-\frac{\kappa}{\upsilon}}\tanh_\Xi\left(\sqrt{-\kappa\upsilon}\Omega\right),$$

$$\zeta_{17}(\Omega) = -\sqrt{-\frac{\kappa}{\upsilon}}\coth_\Xi\left(\sqrt{-\kappa\upsilon}\Omega\right),$$

$$\zeta_{18}(\Omega) = -\sqrt{-\frac{\kappa}{\upsilon}}\left(\tanh_\Xi\left(2\sqrt{-\kappa\upsilon}\Omega\right) + i\mathrm{sech}_\Xi\left(2\sqrt{-\kappa\upsilon}\Omega\right)\right),$$

$$\zeta_{19}(\Omega) = -\sqrt{-\frac{\kappa}{\upsilon}}\left(\coth_\Xi\left(2\sqrt{-\kappa\upsilon}\Omega\right) + \mathrm{csch}_\Xi\left(2\sqrt{-\kappa\upsilon}\Omega\right)\right),$$

and

$$\zeta_{20}(\Omega) = -\frac{1}{2}\sqrt{-\frac{\kappa}{\upsilon}}\left(\tanh_\Xi\left(\frac{1}{2}\sqrt{-\kappa\upsilon}\Omega\right) + \coth_\Xi\left(\frac{1}{2}\sqrt{-\kappa\upsilon}\Omega\right)\right).$$

Family. 5: For $\upsilon = \kappa$ and $\mu = 0$, then we have

$$\zeta_{21}(\Omega) = \tan_\Xi\left(\kappa\Omega\right),$$

$$\zeta_{22}(\Omega) = -\cot_\Xi\left(\kappa\Omega\right),$$

$$\zeta_{23}(\Omega) = \tan_{\Xi}(2\kappa\Omega) + \sec_{\Xi}(2\kappa\Omega),$$
$$\zeta_{24}(\Omega) = -\cot_{\Xi}(2\kappa\Omega) + \csc_{\Xi}(2\kappa\Omega),$$

and

$$\zeta_{25}(\Omega) = \frac{1}{2}\tan_{\Xi}\left(\frac{1}{2}\kappa\Omega\right) - \frac{1}{2}\cot_{\Xi}\left(\frac{1}{2}\kappa\Omega\right).$$

Family. 6: For $\upsilon = -\kappa$ and $\mu = 0$,

$$\zeta_{26}(\Omega) = -\tanh_{\Xi}(\kappa\Omega),$$
$$\zeta_{27}(\Omega) = -\coth_{\Xi}(\kappa\Omega),$$
$$\zeta_{28}(\Omega) = -\tanh_{\Xi}(2\kappa\Omega) + i\,\mathrm{sech}_{\Xi}(2\kappa\Omega),$$
$$\zeta_{29}(\Omega) = -\coth_{\Xi}(2\kappa\Omega) + \mathrm{csch}_{\Xi}(2\kappa\Omega),$$

and

$$\zeta_{30}(\Omega) = -\frac{1}{2}\tanh_{\Xi}\left(\frac{1}{2}\kappa\Omega\right) - \frac{1}{2}\coth_{\Xi}\left(\frac{1}{2}\kappa\Omega\right).$$

Family. 7: For $D = 0$,

$$\zeta_{31}(\Omega) = -2\,\frac{\kappa(\mu\Omega\ln\Xi + 2)}{\mu^2\ln(\Xi)\Omega}.$$

Family. 8: For $\upsilon = 0$, $\mu = \varsigma$, and $\kappa = n\varsigma$ (with $n \neq 0$), then we have

$$\zeta_{32}(\Omega) = \Xi^{\varsigma\Omega} - n.$$

Family. 9: For $\mu = \upsilon = 0$,

$$\zeta_{33}(\Omega) = \kappa\Omega\ln(\Xi).$$

Family. 10: For $\mu = \kappa = 0$,

$$\zeta_{34}(\Omega) = -\frac{1}{\upsilon\Omega\ln(\Xi)}.$$

Family. 11: For $\mu \neq 0$, $\upsilon \neq 0$, and $\kappa = 0$,

$$\zeta_{35}(\Omega) = -\frac{\mu}{\upsilon(\cosh_{\Xi}(\mu\Omega) - \sinh_{\Xi}(\mu\Omega) + 1)},$$

and

$$\zeta_{36}(\Omega) = -\frac{\mu(\cosh_{\Xi}(\mu\Omega) + \sinh_{\Xi}(\mu\Omega))}{\upsilon(\cosh_{\Xi}(\mu\Omega) + \sinh_{\Xi}(\mu\Omega) + 1)}.$$

Family. 12: For $\mu = \varsigma$, $\upsilon = n\varsigma$ (with $n \neq 0$), and $\kappa = 0$,

$$\zeta_{37}(\Omega) = \frac{\Xi^{\varsigma\Omega}}{1 - n\Xi^{\varsigma\Omega}}.$$

In the above solutions, $D = \mu^2 - 4\kappa\upsilon$. The generalised trigonometric and hyperbolic functions are expressed as below:

$$\sin_{\Xi}(\Omega) = \frac{\Xi^{i\Omega} - \Xi^{-i\Omega}}{2i}, \quad \cos_{\Xi}(\Omega) = \frac{\Xi^{i\Omega} + \Xi^{-i\Omega}}{2},$$
$$\sec_{\Xi}(\Omega) = \frac{1}{\cos_{\Xi}(\Omega)}, \quad \csc_{\Xi}(\Omega) = \frac{1}{\sin_{\Xi}(\Omega)},$$
$$\tan_{\Xi}(\Omega) = \frac{\sin_{\Xi}(\Omega)}{\cos_{\Xi}(\Omega)}, \quad \cot_{\Xi}(\Omega) = \frac{\cos_{\Xi}(\Omega)}{\sin_{\Xi}(\Omega)}.$$

Similarly,

$$\sinh_{\mho}(\Omega) = \frac{\Xi^{\Omega} - \Xi^{-\Omega}}{2}, \quad \cosh_{\Xi}(\eta) = \frac{\mho^{\Omega} + \Xi^{-\Omega}}{2},$$
$$sech_{\Xi}(\Omega) = \frac{1}{\cosh_{\Xi}(\Omega)}, \quad csch_{\Xi}(\eta) = \frac{1}{\sinh_{\Xi}(\Omega)},$$
$$\tanh_{\Xi}(\Omega) = \frac{\sinh_{\Xi}(\Omega)}{\cosh_{\Xi}(\Omega)}, \quad \coth_{\Xi}(\Omega) = \frac{\cosh_{\Xi}(\Omega)}{\sinh_{\Xi}(\Omega)}.$$

4. The space-time fractional Phi-4 equation

The conformable space-time fractional Phi-4 equation [32]:

$$ {}_0^{\wedge}D_t^{2\alpha} - {}_0^{\wedge} D_x^{2\beta} + m^2 u + n^3 u = 0, 0 < \alpha, \beta \leq 1, \tag{4.1}$$

${}_0^{\wedge}D_t^{\alpha} u$ indicates the Atangana's conformable fractional derivative of u with respect to t of order α and m, n are real constants. Using the following transformation:

$$u(x,t) = W(\zeta), \zeta = \frac{l}{\beta}(x + \frac{1}{\Gamma(\beta)})^{\beta} - \frac{\lambda}{\alpha}(t + \frac{1}{\Gamma(\alpha)})^{\alpha}. \tag{4.2}$$

Denote the transformation variable as ζ and the constants as l and λ. Formulation (4.2) transforms into an ordinary differential equation, which in turn transforms equation (4.1) into the subsequent nonlinear ordinary differential equation (ODE).

$$\lambda^2 W''(\zeta) - l^2 W''(\zeta) + m^2 W(\zeta) + n W^3(\zeta) = 0. \tag{4.3}$$

By considering the uniform equilibrium between the W'' and W^3 components in (4.3), we can determine the equilibrium number M, which may be expressed as $2M = M + 3$, indicating that $N = 1$. The series solution for (4.3) may be obtained by substituting $M = 1$ [33].

$$W(\Omega) = \sum_{i=-1}^{1} s_i (G(\Omega))^i. \tag{4.4}$$

An equation in field $G(\Omega)$ is derived by substituting (4.4) into (4.3), and collecting any terms that have the same orders as $G(\Omega)$. By assigning a value of zero to its coefficients, the expression may be simplified into a series of nonlinear algebraic equations. The resulting problem is resolved using Maple and yields two classes of solutions:

Case 1.

$$\begin{aligned} l &= \sqrt{\frac{\lambda^2 (\ln(\Xi))^2 \zeta^2 - 4\lambda^2 (\ln(\Xi))^2 \upsilon \kappa - 2m^2}{D}} (\ln(\Xi))^{-1}, \lambda = \lambda, \\ d_{-1} &= -2\frac{m\kappa}{\sqrt{-n(D)}}, d_0 = \sqrt{-\frac{1}{n(D)}}\mu m, d_1 = 0. \end{aligned} \tag{4.5}$$

Case 2.

$$l=\sqrt{\frac{\lambda^{2}(\ln(\Xi))^{2}\zeta^{2}-4\lambda^{2}(\ln(\Xi))^{2}\upsilon\kappa-2m^{2}}{D}}(\ln(\Xi))^{-1},\lambda=\lambda,$$
$$d_{-1}=0,d_{0}=-\frac{m\mu}{\sqrt{-n(D)}},d_{1}=-2\sqrt{-\frac{1}{n(D)}}m\upsilon. \tag{4.6}$$

Using Eq (4.5) and the matching solution of (3.4), we can obtain the following families of kink soliton solutions, assuming Case 1 [34].

Family. 1.1: When $D<0,\ \upsilon\neq 0$, we have,

$$W_{1,1}(x,t)=-2m\kappa\frac{1}{\sqrt{-n(D)}}\left(-\frac{1}{2}\frac{\mu}{\upsilon}+\frac{1}{2}\frac{\sqrt{-D}\tan_{\Xi}\left(\frac{1}{2}\sqrt{-D}\Omega\right)}{\upsilon}\right)^{-1}-\sqrt{-\frac{1}{n(D)}}\mu m, \tag{4.7}$$

$$W_{1,2}(x,t)=-2m\kappa\frac{1}{\sqrt{-n(D)}}\left(-\frac{1}{2}\frac{\mu}{\upsilon}-\frac{1}{2}\frac{\sqrt{-D}\cot_{\Xi}\left(\frac{1}{2}\sqrt{-D}\Omega\right)}{\upsilon}\right)^{-1}-\sqrt{-\frac{1}{n(D)}}\mu m, \tag{4.8}$$

$$W_{1,3}(x,t)=-2m\kappa\frac{1}{\sqrt{-n(D)}}\left(-\frac{1}{2}\frac{\mu}{\upsilon}+\frac{1}{2}\frac{\sqrt{-D}\left(\tan_{\Xi}\left(\sqrt{-D}\Omega\right)\pm\left(\sec_{\Xi}\left(\sqrt{-D}\Omega\right)\right)\right)}{\upsilon}\right)^{-1}-\sqrt{-\frac{1}{n(D)}}\mu m, \tag{4.9}$$

$$W_{1,4}(x,t)=-2m\kappa\frac{1}{\sqrt{-n(D)}}\left(-\frac{1}{2}\frac{\mu}{\upsilon}+\frac{1}{2}\frac{\sqrt{-D}\left(\cot_{\Xi}\left(\sqrt{-D}\Omega\right)\pm\left(\csc_{\Xi}\left(\sqrt{-D}\Omega\right)\right)\right)}{\upsilon}\right)^{-1}-\sqrt{-\frac{1}{n(D)}}\mu m, \tag{4.10}$$

and

$$W_{1,5}(x,t)=-2m\kappa\frac{1}{\sqrt{-n(D)}}\left(-\frac{1}{2}\frac{\mu}{\upsilon}+\frac{1}{4}\frac{\sqrt{-D}\left(\tan_{\Xi}\left(\frac{1}{4}\sqrt{-D}\Omega\right)-\cot_{\Xi}\left(1/4\sqrt{-D}\Omega\right)\right)}{\upsilon}\right)^{-1}-\sqrt{-\frac{1}{n(D)}}\mu m. \tag{4.11}$$

Family. 1.2: When $D > 0,\ \upsilon \neq 0$, then we have

$$W_{1,6}(x,t) = -2\,m\kappa \frac{1}{\sqrt{-n\,(D)}}\left(-\frac{1}{2}\frac{\mu}{\upsilon} - \frac{1}{2}\frac{\sqrt{D}\tanh_{\Xi}\left(\frac{1}{2}\sqrt{-\Delta}\Omega\right)}{\upsilon}\right)^{-1} - \sqrt{-\frac{1}{n\,(D)}}\mu\, m, \tag{4.12}$$

$$W_{1,7}(x,t) = -2\,m\kappa \frac{1}{\sqrt{-n\,(D)}}\left(-\frac{1}{2}\frac{\zeta}{\upsilon} - \frac{1}{2}\frac{\sqrt{D}\coth_{\Xi}\left(\frac{1}{2}\sqrt{-D}\Omega\right)}{\upsilon}\right)^{-1} + \sqrt{-\frac{1}{n\,(D)}}\mu\, m, \tag{4.13}$$

$$W_{1,8}(x,t) = -2\,m\kappa \frac{1}{\sqrt{-n\,(D)}}\left(-\frac{1}{2}\frac{\mu}{\upsilon} + \frac{1}{2}\frac{\sqrt{D}\left(\tanh\left(\sqrt{-D}\Omega\right) \pm \left(sech_{\Xi}\left(\sqrt{-D}\Omega\right)\right)\right)}{\upsilon}\right)^{-1} - \sqrt{-\frac{1}{n\,(D)}}\mu\, m, \tag{4.14}$$

$$W_{1,9}(x,t) = -2\,m\kappa \frac{1}{\sqrt{-n\,(D)}}\left(-\frac{1}{2}\frac{\mu}{\upsilon} + \frac{1}{2}\frac{\sqrt{D}\left(\coth_{\Xi}\left(\sqrt{-D}\Omega\right) \pm \left(sech_{\Xi}\left(\sqrt{-D}\Omega\right)\right)\right)}{\upsilon}\right)^{-1} - \sqrt{-\frac{1}{n\,(D)}}\mu\, m, \tag{4.15}$$

$$W_{1,10}(x,t) = -2\,m\kappa \frac{1}{\sqrt{-n\,(D)}}\left(-\frac{1}{2}\frac{\mu}{\upsilon} - \frac{1}{4}\frac{\sqrt{D}\left(\tanh_{\Xi}\left(1/4\sqrt{D}\Omega\right) - \coth_{\Xi}\left(\frac{1}{4}\sqrt{D}\Omega\right)\right)}{\upsilon}\right)^{-1} - \sqrt{-\frac{1}{n\,(D)}}\mu\, m. \tag{4.16}$$

Family. 1.3: If $\mu = 0$ and $\kappa\upsilon > 0$, then we have

$$W_{1,11}(x,t) = -2\,m\kappa \frac{1}{\sqrt{-n\,(D)}}\frac{1}{\sqrt{\frac{\kappa}{\upsilon}}}\left(\tan_{\Xi}\left(\sqrt{\kappa\,\upsilon}\Omega\right)\right)^{-1}, \tag{4.17}$$

$$W_{1,12}(x,t) = 2\,m\kappa \frac{1}{\sqrt{-n\,(D)}}\frac{1}{\sqrt{\frac{\kappa}{\upsilon}}}\left(\cot_{\Xi}\left(\sqrt{\kappa\,\upsilon}\Omega\right)\right)^{-1}, \tag{4.18}$$

$$W_{1,13}(x,t) = -2\,m\kappa \frac{1}{\sqrt{-n\,(D)}}\frac{1}{\sqrt{\frac{\kappa}{\upsilon}}}\left(\tan_{\Xi}\left(2\sqrt{\kappa\,\upsilon}\Omega\right) \pm \left(\sec_{\Xi}\left(2\sqrt{\kappa\,\upsilon}\Omega\right)\right)\right)^{-1}, \tag{4.19}$$

$$W_{1,14}(x,t) = 2\,m\kappa \frac{1}{\sqrt{-n\,(D)}}\frac{1}{\sqrt{\frac{\kappa}{\upsilon}}}\left(\cot_{\Xi}\left(2\sqrt{\kappa\,\upsilon}\Omega\right) \pm \left(\csc_{\Xi}\left(2\sqrt{\kappa\,\upsilon}\Omega\right)\right)\right)^{-1}, \tag{4.20}$$

and

$$W_{1,15}(x,t) = -4\,m\kappa \frac{1}{\sqrt{-n\,(D)}}\frac{1}{\sqrt{\frac{\kappa}{\upsilon}}}\left(\tan_{\Xi}\left(\frac{1}{2}\sqrt{\kappa\,\upsilon}\Omega\right) - \cot_{\Xi}\left(\frac{1}{2}\sqrt{\kappa\,\upsilon}\Omega\right)\right)^{-1}. \tag{4.21}$$

Family. 1.4: When $\upsilon\kappa < 0$ and $\mu = 0$, then we have

$$W_{1,16}(x,t) = 2\,m\kappa \frac{1}{\sqrt{-n\,(D)}} \frac{1}{\sqrt{-\frac{\kappa}{\upsilon}}} \left(\tanh \Xi \left(\sqrt{-\kappa\,\upsilon}\Omega\right)\right)^{-1}, \tag{4.22}$$

$$W_{1,17}(x,t) = 2\,m\kappa \frac{1}{\sqrt{-n\,(D)}} \frac{1}{\sqrt{-\frac{\kappa}{\upsilon}}} \left(\cot_{\Xi} \left(\sqrt{-\kappa\,\upsilon}\Omega\right)\right)^{-1}, \tag{4.23}$$

$$W_{1,18}(x,t) = 2\,m\kappa \frac{1}{\sqrt{-n\,(D)}} \frac{1}{\sqrt{-\frac{\kappa}{\upsilon}}} \left(\tanh_{\Xi} \left(2\, \sqrt{-\kappa\,\upsilon}\Omega\right) \pm \left(isech\left(2\, \sqrt{-\kappa\,\upsilon}\Omega\right)\right)\right)^{-1}, \tag{4.24}$$

$$W_{1,19}(x,t) = 2\,m\kappa \frac{1}{\sqrt{-n\,(D)}} \frac{1}{\sqrt{-\frac{\kappa}{\upsilon}}} \left(\coth_{\Xi} \left(2\, \sqrt{-\kappa\,\upsilon}\Omega\right) \pm \left(csch_{\Xi}\left(2\, \sqrt{-\kappa\,\upsilon}\Omega\right)\right)\right)^{-1}, \tag{4.25}$$

and

$$W_{1,20}(x,t) = 4\,m\kappa \frac{1}{\sqrt{-n\,(D)}} \frac{1}{\sqrt{-\frac{\kappa}{\upsilon}}} \left(\tanh_{\Xi} \left(\frac{1}{2}\, \sqrt{-\kappa\,\upsilon}\Omega\right) + \coth_{\Xi}\left(\frac{1}{2}\, \sqrt{-\kappa\,\upsilon}\Omega\right)\right)^{-1}. \tag{4.26}$$

Family. 1.5: When $\upsilon = \kappa$ and $\mu = 0$, then we have

$$W_{1,21}(x,t) = -2\,\frac{m\kappa}{\sqrt{-n\,(D)}\tan_{\Xi}(\kappa\,\Omega)}, \tag{4.27}$$

$$W_{1,22}(x,t) = 2\,\frac{m\kappa}{\sqrt{-n\,(D)}_{\Xi}(\eta\,\Omega)}, \tag{4.28}$$

$$W_{1,23}(x,t) = -2\,\frac{m\kappa}{\sqrt{-n\,(D)}\,(\tan_{\Xi}(2\,\kappa\,\Omega) \pm (\sec_{\Xi}(2\,\kappa\,\Omega)))}, \tag{4.29}$$

$$W_{1,24}(x,t) = -2\,\frac{m\kappa}{\sqrt{-n\,(D)}\,(-\cot_{\Xi}(2\,\kappa\,\Omega) \pm (\csc_{\Xi}(2\,\kappa\,\Omega)))}, \tag{4.30}$$

and

$$W_{1,25}(x,t) = -2\,\frac{m\kappa}{\sqrt{-n\,(D)}\left(\frac{1}{2}\tan_{\Xi}\left(\frac{1}{2}\kappa\,\Omega\right) - \frac{1}{2}\cot_{\Xi}\left(\frac{1}{2}\kappa\,\Omega\right)\right)}. \tag{4.31}$$

Family. 1.6: When $\upsilon = -\kappa$ and $\mu = 0$, then we have

$$w_{1,26}(x,t) = 2\,\frac{m\kappa}{\sqrt{-n\,(D)}\tanh_{\Xi}(\kappa\,\Omega)}, \tag{4.32}$$

$$W_{1,27}(x,t) = 2\,\frac{m\kappa}{\sqrt{-n\,(D)}\coth_{\Xi}(\kappa\,\Omega)}, \tag{4.33}$$

$$W_{1,28}(x,t) = -2\,\frac{m\kappa}{\sqrt{-n\,(D)}\,(-\tanh_{\Xi}(2\,\kappa\,\Omega) \pm (isech_{\Xi}(2\,\kappa\,\Omega)))}, \tag{4.34}$$

$$W_{1,29}(x,t) = -2\,\frac{m\kappa}{\sqrt{-n\,(D)}\,(-\coth_{\Xi}(2\,\kappa\,\Omega) \pm (cech_{\Xi}(2\,\kappa\,\Omega)))}, \tag{4.35}$$

and

$$W_{1,30}(x,t) = -2\,\frac{m\kappa}{\sqrt{-n\,(D)}\left(-\frac{1}{2}\tanh_{\Xi}\left(\frac{1}{2}\kappa\,\Omega\right) - \frac{1}{2}coth_{\Xi}\left(\frac{1}{2}\kappa\,\Omega\right)\right)}. \tag{4.36}$$

Family. 1.7: When $\mu = \varsigma$, $\kappa = \tau\varsigma(\tau \neq 0)$, and $\upsilon = 0$,

$$W_{1,31}(x,t) = -2\,\frac{m\tau\,\varsigma\,(\tau \neq 0)}{\sqrt{-n\,(D)}\,(\Xi^{\varsigma\,\Omega} - \tau)} + \sqrt{-\frac{1}{n\,(D)}}\varsigma\,m. \tag{4.37}$$

Family. 1.8: When $\mu = \upsilon = 0$, then we have

$$W_{1,32}(x,t) = -2\,\frac{m}{\sqrt{-n\,(D)}\Omega i\,\ln\,(\Xi)}. \tag{4.38}$$

Family. 1.9: When $\mu \neq 0,\ \upsilon \neq 0,\ \kappa = 0$,

$$w_{1,33}(x,t) = \sqrt{-\frac{1}{n\,(D)}}\mu\,m, \tag{4.39}$$

$$w_{1,34}(x,t) = \sqrt{-\frac{1}{n\,(D)}}\mu\,m. \tag{4.40}$$

Family. 1.10: When $\mu = \varsigma,\ \upsilon = \tau,\ \kappa = 0$,

$$w_{1,35}(x,t) = \sqrt{-\frac{1}{n\,(D)}}\varsigma\,m. \tag{4.41}$$

Assuming Case 2, we have

Family. 2.1: When $D < 0\ \upsilon \neq 0$,

$$\begin{aligned} W_{2,1}(x,t) = -2\,m\upsilon&\left(-\frac{1}{2}\frac{\mu}{\upsilon} + \frac{1}{2}\frac{\sqrt{-D}\tan_{\Xi}\left(\frac{1}{2}\sqrt{-D}\Omega\right)}{\upsilon}\right)\frac{1}{\sqrt{-n\,(D)}} \\ &- \sqrt{-\frac{1}{n\,(D)}}\mu\,m, \end{aligned} \tag{4.42}$$

$$\begin{aligned} W_{2,2}(x,t) = -2\,m\upsilon&\left(-\frac{1}{2}\frac{\mu}{\upsilon} - \frac{1}{2}\frac{\sqrt{-D}\cot_{\Xi}\left(\frac{1}{2}\sqrt{-D}\Omega\right)}{\upsilon}\right)\frac{1}{\sqrt{-n\,(D)}} \\ &- \sqrt{-\frac{1}{n\,(D)}}\mu\,m, \end{aligned} \tag{4.43}$$

$$\begin{aligned} W_{2,3}(x,t) = -2\,m\upsilon&\left(-\frac{1}{2}\frac{\mu}{\upsilon} + \frac{1}{2}\frac{\sqrt{-D}\left(\tan_{\Xi}\left(\sqrt{-D}\Omega\right) \pm \left(\sec_{\Xi}\left(\sqrt{-D}\Omega\right)\right)\right)}{\upsilon}\right)\frac{1}{\sqrt{-n\,(D)}} \\ &- \sqrt{-\frac{1}{n\,(D)}}\mu\,m, \end{aligned} \tag{4.44}$$

$$W_{2,4}(x,t) = -2\,m\upsilon\left(-\frac{1}{2}\frac{\mu}{\upsilon} + \frac{1}{2}\frac{\sqrt{-D}\left(\cot_{\Xi}\left(\sqrt{-D}\Omega\right) \pm \left(\csc_{\Xi}\left(\sqrt{-D}\Omega\right)\right)\right)}{\upsilon}\right)\frac{1}{\sqrt{-n\,(D)}} - \sqrt{-\frac{1}{n\,(D)}}\mu\,m, \tag{4.45}$$

$$W_{2,5}(x,t) = -2\,m\upsilon\left(-\frac{1}{2}\frac{\mu}{\upsilon} + \frac{1}{4}\frac{\sqrt{-D}\left(\tan_{\Xi}\left(\frac{1}{4}\sqrt{-D}\Omega\right) - \cot_{\Xi}\left(\frac{1}{4}\sqrt{-D}\Omega\right)\right)}{\upsilon}\right)\frac{1}{\sqrt{-n\,(D)}} - \sqrt{-\frac{1}{n\,(D)}}\mu\,m. \tag{4.46}$$

Family. 2.2: When $D > 0,\ \upsilon \neq 0$,

$$W_{2,6}(x,t) = -2\,m\upsilon\left(-\frac{1}{2}\frac{\mu}{\upsilon} - \frac{1}{2}\frac{\sqrt{D}\tanh_{\Xi}\left(\frac{1}{2}\sqrt{-\Delta}\Omega\right)}{\upsilon}\right)\frac{1}{\sqrt{-n\,(D)}} - \sqrt{-\frac{1}{n\,(D)}}\mu\,m, \tag{4.47}$$

$$W_{2,7}(x,t) = -2\,m\upsilon\left(-\frac{1}{2}\frac{\mu}{\upsilon} - \frac{1}{2}\frac{\sqrt{D}\coth_{\Xi}\left(\frac{1}{2}\sqrt{-D}\Omega\right)}{\upsilon}\right)\frac{1}{\sqrt{-n\,(D)}} + \sqrt{-\frac{1}{n\,(D)}}\mu\,m, \tag{4.48}$$

$$W_{2,8}(x,t) = -2\,m\upsilon\left(-\frac{1}{2}\frac{\mu}{\upsilon} + \frac{1}{2}\frac{\sqrt{D}\left(\tanh_{\Xi}\left(\sqrt{-D}\Omega\right) \pm \left(sech_{\Xi}\left(\sqrt{-D}\Omega\right)\right)\right)}{\upsilon}\right)\frac{1}{\sqrt{-n\,(D)}} - \sqrt{-\frac{1}{n\,(D)}}\mu\,m, \tag{4.49}$$

$$W_{2,9}(x,t) = -2\,m\upsilon\left(\frac{-1}{2}\frac{\mu}{\upsilon} + \frac{1}{2}\frac{\sqrt{D}\left(\coth_{\Xi}\left(\sqrt{-D}\Omega\right) \pm \left(sech_{\Xi}\left(\sqrt{-D}\Omega\right)\right)\right)}{\upsilon}\right)\frac{1}{\sqrt{-n\,(D)}} - \sqrt{-\frac{1}{n\,(D)}}\mu\,m, \tag{4.50}$$

and

$$W_{2,10}(x,t) = -2\,m\upsilon\left(-\frac{1}{2}\frac{\mu}{\upsilon} - \frac{1}{4}\frac{\sqrt{D}\left(\tanh_{\Xi}\left(\frac{1}{4}\sqrt{D}\Omega\right) - \coth_{\Xi}\left(\frac{1}{4}\sqrt{D}\Omega\right)\right)}{\upsilon}\right)\frac{1}{\sqrt{-n\,(D)}} - \sqrt{-\frac{1}{n\,(D)}}\mu\,m. \tag{4.51}$$

Family. 2.3: When $\kappa\upsilon > 0$ and $\mu = 0$,

$$W_{2,11}(x,t) = -2\,m\upsilon\,\sqrt{\frac{\kappa}{\upsilon}}\tan_{\Xi}\left(\sqrt{\upsilon\,\kappa}\Omega\right)\frac{1}{\sqrt{-n\,(D)}}, \tag{4.52}$$

$$W_{2,12}(x,t) = 2\,m\upsilon\,\sqrt{\frac{\kappa}{\upsilon}}\cot_{\Xi}\left(\sqrt{\upsilon\,\kappa}\Omega\right)\frac{1}{\sqrt{-n\,(D)}}, \tag{4.53}$$

$$W_{2,13}(x,t) = -2\,m\upsilon\,\sqrt{\frac{\kappa}{\upsilon}}\left(\tan_{\Xi}\left(2\,\sqrt{\upsilon\,\kappa}\Omega\right) \pm \left(\sec_{\Xi}\left(2\,\sqrt{\upsilon\,\kappa}\Omega\right)\right)\right)\frac{1}{\sqrt{-n\,(D)}}, \tag{4.54}$$

$$W_{2,14}(x,t) = 2\,m\upsilon\,\sqrt{\frac{\kappa}{\upsilon}}\left(\cot_{\Xi}\left(2\,\sqrt{\upsilon\,\kappa}\Omega\right) \pm \left(\csc_{\Xi}\left(2\,\sqrt{\upsilon\,\kappa}\Omega\right)\right)\right)\frac{1}{\sqrt{-n\,(D)}}, \tag{4.55}$$

and

$$W_{2,15}(x,t) = -m\upsilon\,\sqrt{\frac{\kappa}{\upsilon}}\left(\tan_{\Xi}\left(\frac{1}{2}\,\sqrt{\upsilon\,\kappa}\Omega\right) - \cot_{\Xi}\left(\frac{1}{2}\,\sqrt{\upsilon\,\kappa}\Omega\right)\right)\frac{1}{\sqrt{-n\,(D)}}. \tag{4.56}$$

Family. 2.4: When $\upsilon\kappa < 0$ and $\mu = 0$,

$$W_{2,16}(x,t) = 2\,m\upsilon\,\sqrt{-\frac{\kappa}{\upsilon}}\tanh\left(\sqrt{-\upsilon\,\kappa}\Omega\right)\frac{1}{\sqrt{-n\,(D)}}, \tag{4.57}$$

$$W_{2,17}(x,t) = 2\,m\upsilon\,\sqrt{-\frac{\kappa}{\upsilon}}\coth_{\Xi}\left(\sqrt{-\upsilon\,\kappa}\Omega\right)\frac{1}{\sqrt{-n\,(D)}}, \tag{4.58}$$

$$w_{2,18}(x,t) = 2\,m\upsilon\,\sqrt{-\frac{\kappa}{\upsilon}}\left(\tanh_{\Xi}\left(2\,\sqrt{-\upsilon\,\kappa}\Omega\right) \pm \left(isech_{\Xi}\left(2\,\sqrt{-\upsilon\,\kappa}\Omega\right)\right)\right)\frac{1}{\sqrt{-n\,(D)}}, \tag{4.59}$$

$$W_{2,19}(x,t) = 2\,m\upsilon\,\sqrt{-\frac{\kappa}{\upsilon}}\left(\coth_{\Xi}\left(2\,\sqrt{-\upsilon\,\kappa}\Omega\right) \pm \left(csch_{\Xi}\left(2\,\sqrt{-\upsilon\,\kappa}\Omega\right)\right)\right)\frac{1}{\sqrt{-n\,(D)}}, \tag{4.60}$$

and

$$W_{2,20}(x,t) = m\upsilon\,\sqrt{-\frac{\kappa}{\upsilon}}\left(\tanh_{\Xi}\left(\frac{1}{2}\,\sqrt{-\upsilon\,\kappa}\Omega\right) + \coth_{\Xi}\left(\frac{1}{2}\,\sqrt{-\upsilon\,\kappa}\Omega\right)\right)\frac{1}{\sqrt{-n\,(D)}}, \tag{4.61}$$

Family. 2.5: When $\upsilon = \kappa$ and $\mu = 0$,

$$W_{2,21}(x,t) = -2\,\frac{m\kappa\,\tan_{\Xi}\left(\kappa\,\Omega\right)}{\sqrt{-n\,(D)}}, \tag{4.62}$$

$$W_{2,22}(x,t) = 2\,\frac{m\kappa\,\cot_{\Xi}\left(\eta\,\Omega\right)}{\sqrt{-n\,(D)}}, \tag{4.63}$$

$$W_{2,23}(x,t) = -2\,\frac{m\kappa\,\left(\tan\left(2\,\kappa\,\psi\right) \pm \left(\sec_{\Xi}\left(2\,\kappa\,\Omega\right)\right)\right)}{\sqrt{-n\,(D)}}, \tag{4.64}$$

$$W_{2,24}(x,t) = -2\,\frac{m\kappa\,\left(-\cot_{\Xi}\left(2\,\kappa\,\Omega\right) \pm \left(\csc_{\Xi}\left(2\,\kappa\,\Omega\right)\right)\right)}{\sqrt{-n\,(D)}}, \tag{4.65}$$

and

$$W_{2,25}(x,t) = -2\,\frac{m\kappa}{\sqrt{-n\,(D)}\left(\frac{1}{2}\tan_{\Xi}\left(\frac{1}{2}\kappa\,\Omega\right) - \frac{1}{2}\cot_{\Xi}\left(\frac{1}{2}\kappa\,\Omega\right)\right)}. \tag{4.66}$$

Family. 2.6: When $\nu = -\eta$ and $\mu = 0$,

$$W_{2,26}(x,t) = 2\,\frac{m\kappa\,\tanh_{\Xi}(\kappa\,\Omega)}{\sqrt{-n\,(D)}}, \tag{4.67}$$

$$W_{2,27}(x,t) = 2\,\frac{m\kappa}{\sqrt{-n\,(D)}\coth_{\Xi}(\kappa\,\Omega)}, \tag{4.68}$$

$$W_{2,28}(x,t) = -2\,\frac{m\kappa\,\left(-\tanh_{\Xi}(2\,\kappa\,\Omega) \pm (isech_{\Xi}(2\,\kappa\,\Omega))\right)}{\sqrt{-n\,(D)}}, \tag{4.69}$$

$$W_{2,29}(x,t) = -2\,\frac{m\kappa\,\left(-\coth_{\Xi}(2\,\kappa\,\Omega) \pm (cech_{\Xi}(2\,\kappa\,\Omega))\right)}{\sqrt{-n\,(D)}}, \tag{4.70}$$

and

$$W_{2,30}(x,t) = -2\,\frac{m\kappa\,\left(-\frac{1}{2}\tanh_{\Xi}\left(\frac{1}{2}\kappa\,\Omega\right) - \frac{1}{2}\coth_{\Xi}\left(\frac{1}{2}\kappa\,\Omega\right)\right)}{\sqrt{-n\,(D)}}. \tag{4.71}$$

Family. 2.7: When $\mu = \varsigma$, $\kappa = \tau\varsigma(\tau \neq 0)$, and $\upsilon = 0$,

$$W_{2,31}(x,t) = -\sqrt{-\frac{1}{n\,(D)}}\varsigma\,m. \tag{4.72}$$

Family. 2.8: When $\mu = \upsilon = 0$,

$$W_{2,32}(x,t) = -2\,\frac{m}{\sqrt{-n\,(D)}\Omega\,\ln(\Xi)}. \tag{4.73}$$

Family. 2.9: When $\mu \neq 0, \upsilon \neq 0, \kappa = 0$,

$$w_{2,33}(x,t) = 2\,\frac{m\mu}{\sqrt{-n\,(D)}\,(\cosh(\mu\,\Omega) - \sinh(\mu\,\Omega) + 1)} - \sqrt{-\frac{1}{n\,(D)}}\mu\,m, \tag{4.74}$$

$$w_{2,34}(x,t) = 2\,\frac{m\mu\,(\cosh(\mu\,\Omega) + \sinh(\mu\,\Omega))}{\sqrt{-n\,(D)}\,(\cosh(\mu\,\Omega) + \sinh(\mu\,\Omega) + 1)} - \sqrt{-\frac{1}{n\,(D)}}\mu\,m. \tag{4.75}$$

Family.2.10: When $\mu = \varsigma, \upsilon = \tau, \kappa = 0$,

$$w_{2,35}(x,t) = 2\,\frac{m\tau\,\varsigma\,\Xi^{\varsigma\,\Omega}}{\sqrt{-n\,(D)}\,(1 - \tau\,\Xi^{\varsigma\,\Omega})} - \sqrt{-\frac{1}{n\,(D)}}\varsigma\,m. \tag{4.76}$$

5. Discussions

To the best of our knowledge, the usage of mEDAM with the STFP4E has not been verified in any scientific paper. In order to generate wave structures in both 3D and contour forms, this study uses the improved EDAM version, known as NEDAM, to generate graphical representations of the many wave types seen in the system. Notably, our findings demonstrate the important existence of various kink configurations, which are crucial for comprehending how physical processes are interrelated.Our results are intended to improve understanding of soliton solutions associated with processes of temporal evolution. According to the findings, kink soliton formations—which often display coherent structures inside reaction-diffusion systems—can only be observed using the STFP4E framework.Key dynamics are depicted in the figures: Figure 1 shows how solitons form, oscillate, and disperse in a nonlinear medium. The spatial evolution of the soliton, highlighting compression and decay, is depicted in Figure 2. Figure 4 shows how frequency influences wave intensity, exposing variances in strength, while Figure 3 shows how the wave packet's structure varies. The energy distribution at various frequencies is shown in Figure 5, and the energy distribution and spatial evolution are combined in Figure 6. Finally, Figure 7 illustrates the intensity and frequency changes of a wave as it moves across space, and Figure 8 displays the concentration and dissipation of a laser beam. In conclusion, this study shows how well NEDAM works to solve challenging issues in a variety of scientific domains while also providing insightful information on the dynamics of nonlinear systems.The study's conclusions stand out due to the data's unambiguous demonstration of the important inclusion of different types of kink structures.

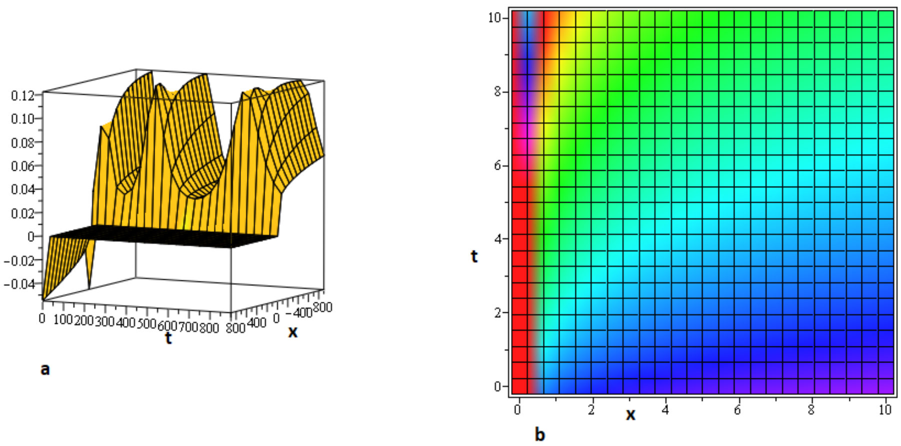

Figure 1. The three-dimensional and contour visuals of the 3-kink soliton solution $w_{1,1}$ stated in (20) are graphed for $\kappa := 1, \mu := .1, \upsilon := 11, Xi := 1, \beta := .156, \alpha = .155, n = 1, m = .1. l = 1, \lambda = .1$. While two-dimensional visual is simultaneously graphed for $t = 0$ and for the same values of involved parameters.

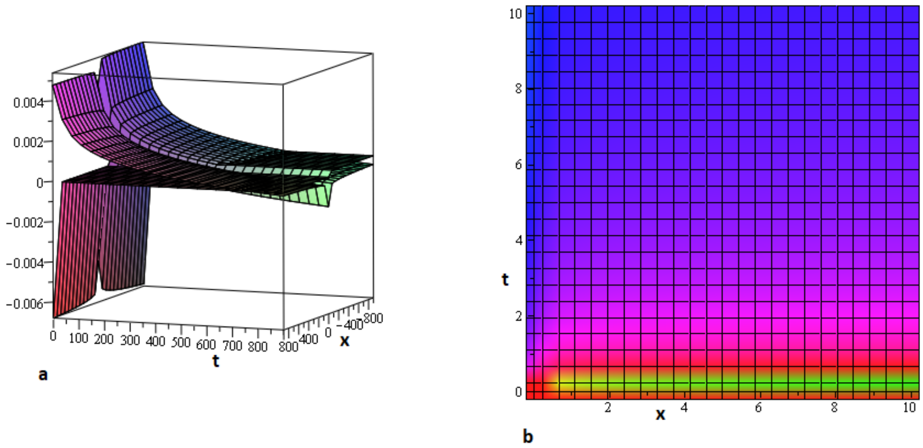

Figure 2. The three-dimensional and contour visuals of the 3-kink soliton solution $w_{1,1}$ stated in (21) are graphed for $\kappa := 1, \mu := .1, \upsilon := 11, Xi := 1, \beta := .156, \alpha = .155, n = 1, m = .1.l = 1, \lambda = .1$. While two-dimensional visual is simultaneously graphed for $t = 0$ and for the same values of involved parameters.

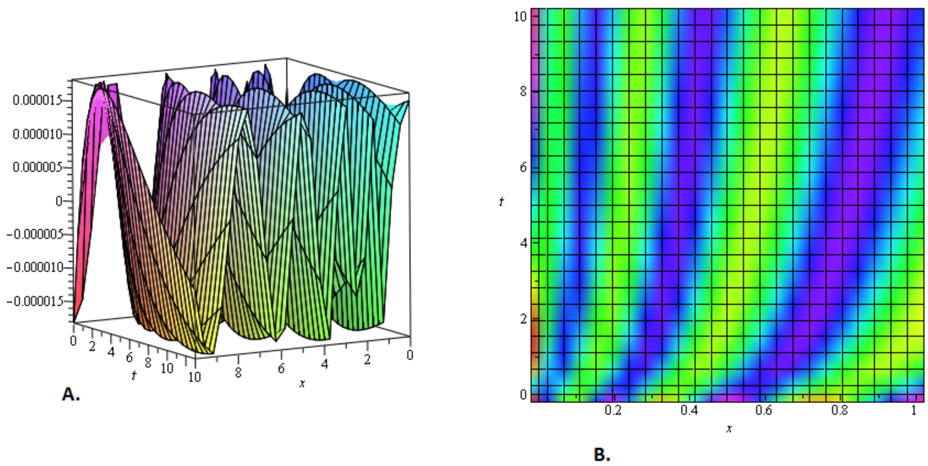

Figure 3. The three-dimensional and contour visuals of the 3-kink soliton solution $w_{1,1}$ stated in (25) are graphed for $\kappa := 1, \mu := .1, \upsilon := 11, Xi := 1, \beta := .156, \alpha = .155, n = 1, m = .1.l = 1, \lambda = .1$. While two-dimensional visual is simultaneously graphed for $t = 0$ and for the same values of involved parameters.

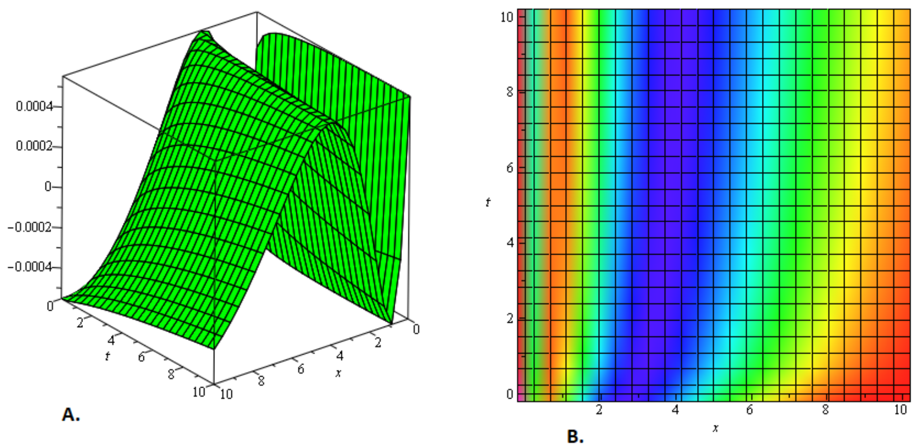

Figure 4. The three-dimensional and contour visuals of the 3-kink soliton solution $w_{1,1}$ stated in (26) are graphed for $\kappa := .1, \mu := 11, \upsilon := .11, Xi := 1, \beta := .156, \alpha = .155, n = 1, m = .1.l = 1, \lambda = .1$. While two-dimensional visual is simultaneously graphed for $t = 0$ and for the same values of involved parameters.

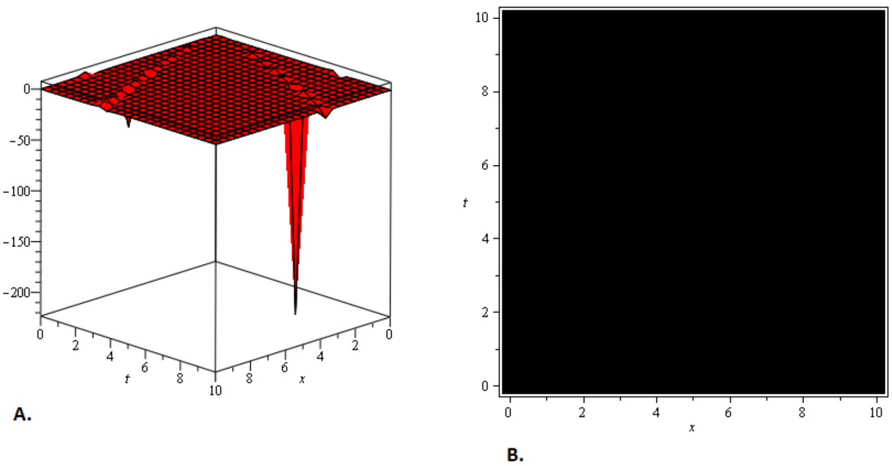

Figure 5. The three-dimensional and contour visuals of the 3-kink soliton solution $w_{1,1}$ stated in (55) are graphed for $\kappa := .11, \mu := 2, \upsilon := .1, Xi := 1, \beta := .156, \alpha = .155, n = 1, m = .1.l = .11, \lambda = .11$. While two-dimensional visual is simultaneously graphed for $t = 0$ and for the same values of involved parameters.

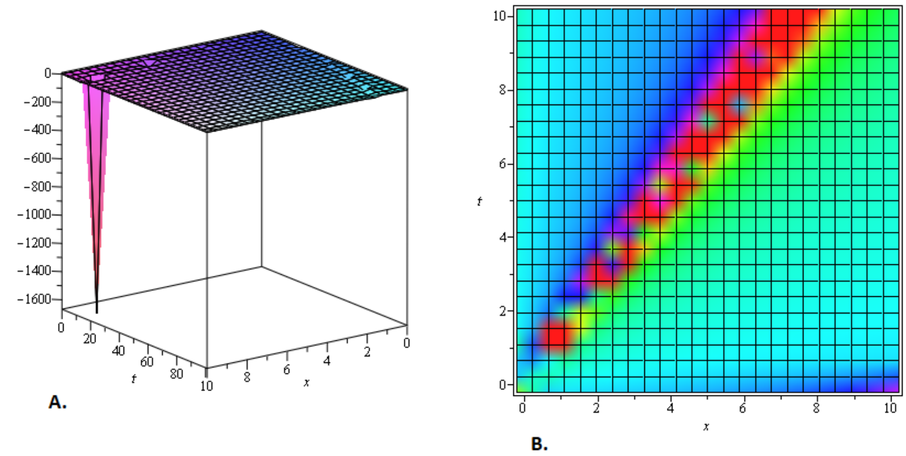

Figure 6. The three-dimensional and contour visuals of the 3-kink soliton solution $w_{1,1}$ stated in (60) are graphed for $\kappa := 1, \mu := 11, \upsilon := 1, Xi := 1, \beta := .156, \alpha = .155, n = .1, m = .1.l = .11, \lambda = .111$. While two-dimensional visual is simultaneously graphed for $t = 0$ and for the same values of involved parameters.

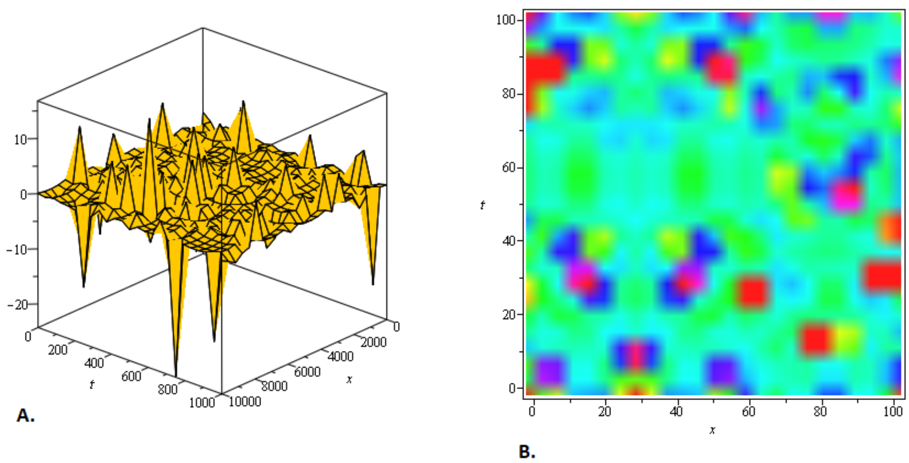

Figure 7. The three-dimensional and contour visuals of the 3-kink soliton solution $w_{1,1}$ stated in (61) are graphed for $\kappa := 0, \mu := 22, \upsilon := 2, Xi := 1, \beta := 2, \alpha = .55, n = .1, m = .1.l = .2, \lambda = 1$. While two-dimensional visual is simultaneously graphed for $t = 0$ and for the same values of involved parameters.

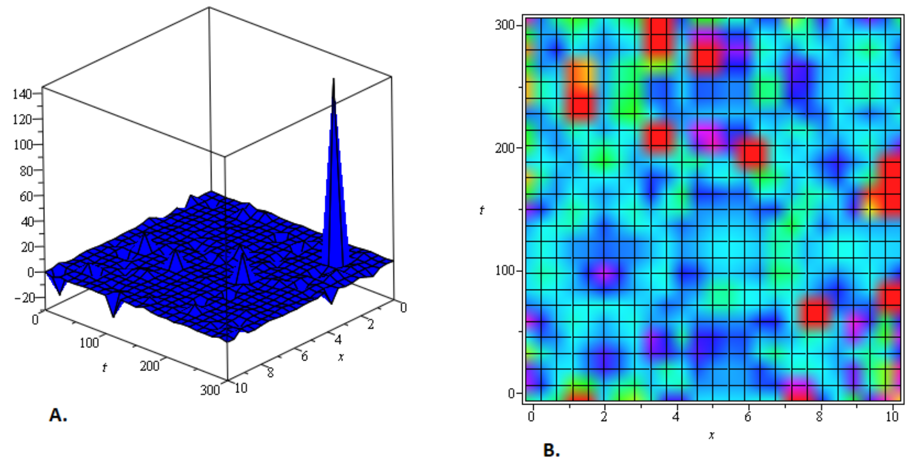

Figure 8. The three-dimensional and contour visuals of the 3-kink soliton solution $w_{1,1}$ stated in (75) are graphed for $\kappa := 222, \mu := 0, \upsilon := 222, Xi := 1, \beta := 2, \alpha = .5, n = 1, m = .1.l = .11, \lambda = 1$. While two-dimensional visual is simultaneously graphed for $t = 0$ and for the same values of involved parameters.

6. Conclusions

This work investigates soliton propagation in STP4E by means of the mEDAM and ABD techniques. We first correctly translate the equation into a nonlinear ordinary differential equation (NODE), and then, we build families of soliton solutions for generalised exponential, hyperbolic, trigonometric, and rational functions by assuming a series-form solution. Graphical representations of the spreading behaviour of different soliton solutions can be produced using contour, 3D, and 2D graphs. These results are very helpful in studying propagation processes and have applications in the mathematics field. Without a doubt, the application of mEDAM greatly enhanced our comprehension of soliton dynamics, nonlinear dynamics, and the connection between these and the STP4E. This increases the likelihood that more research in these areas will be possible. On the other hand, when there is an imbalance, the method becomes troublesome.

Author contributions

Ikram Ullah: conceptualization, methodology, writing-driginal draft; Muhammad Bilal, Aditi Sharma, Shivam Bhardwaj: formal analysis, validation, software, visualization, review & editing; Hasim Khan, Sunil Kumar Sharma: mathematical modeling, data curation, mathematics-related tasks, writing-review & editing.

All authors have read and approved the final version of the manuscript for publication.

Acknowledgments

The author extends the appreciation to the Deanship of Postgraduate Studies and Scientific Research at Majmaah University for funding this research work through the project number (ICR-2024-1378). We also acknowledge Central South University China for its support through the TAS research laboratory.

Conflict of interest

The authors declare no conflict of interest.

References

1. A. Khan, T. Abdeljawad, J. F. Gomez-Aguilar, H. Khan, Dynamical study of fractional order mutualism parasitism food web module, *Chaos Soliton. Fract.*, **134** (2020), 109685. https://doi.org/10.1016/j.chaos.2020.109685
2. M. Aslam, R. Murtaza, T. Abdeljawad, G. U. Rahman, A. Khan, H. Khan, et al., A fractional order HIV/AIDS epidemic model with Mittag-Leffler kernel, *Adv. Differ. Equ.*, **2021** (2021), 107. https://doi.org/10.1186/s13662-021-03264-5
3. H. Khan, Z. A. Khan, H. Tajadodi, A. Khan, Existence and data-dependence theorems for fractional impulsive integro-differential system, *Adv. Differ. Equ.*, **2020** (2020), 458. https://doi.org/10.1186/s13662-020-02823-6
4. A. Khan, H. Khan, J. F. Gómez-Aguilar, T. Abdeljawad, Existence and Hyers-Ulam stability for a nonlinear singular fractional differential equations with Mittag-Leffler kernel, *Chaos Soliton. Fract.*, **127** (2019), 422–427. https://doi.org/10.1016/j.chaos.2019.07.026
5. A. Khan, P. S. Scindia, S. T. Sutar, T. Abdeljawad, On stability analysis of a fractional volterra integro delay differential equation in the context of Mittag-Leffler kernel, *Wave. Random Complex*, **2023** (2023), 1–19. https://doi.org/10.1080/17455030.2023.2223720
6. H. Khan, J. Alzabut, H. Gulzar, Existence of solutions for hybrid modified ABC-fractional differential equations with p-Laplacian operator and an application to a waterborne disease model, *Alex. Eng. J.*, **70** (2023), 665–672. https://doi.org/10.1016/j.aej.2023.02.045
7. A. Berhail, N. Tabouche, M. M. Matar, J. Alzabut, On nonlocal integral and derivative boundary value problem of nonlinear Hadamard Langevin equation with three different fractional orders, *Bol. Soc. Mat. Mex.*, **26** (2020), 303–318. https://doi.org/10.1007/s40590-019-00257-z
8. M. Bilal, J. Iqbal, K. Shah, B. Abdalla, T. Abdeljawad, I. Ullah, Analytical solutions of the space-time fractional Kundu-Eckhaus equation by using modified extended direct algebraic method, *Partial Differential Equations in Applied Mathematics*, **11** (2024), 100832. https://doi.org/10.1016/j.padiff.2024.100832
9. V. F. Morales-Delgado, M. A. Taneco-Hernández, J. F. Gómez-Aguilar, On the solutions of fractional order of evolution equations, *Eur. Phys. J. Plus*, **132** (2017), 47. https://doi.org/10.1140/epjp/i2017-11341-0

10. A. Atangana, J. F. Gómez-Aguilar, Decolonisation of fractional calculus rules: Breaking commutativity and associativity to capture more natural phenomena, *Eur. Phys. J. Plus*, **133** (2018), 166. https://doi.org/10.1140/epjp/i2018-12021-3
11. E. M. E. Zayed, Y. A. Amer, A. H. Arnous, Functional variable method and its applications for finding exact solutions of nonlinear PDEs in mathematical physics, *Sci. Res. Essays*, **8** (2013), 2068–2074.
12. Y. Yıldırım, A. Biswas, M. Asma, P. Guggilla, S. Khan, M. Ekici, et al., Pure-cubic optical soliton perturbation with full nonlinearity, *Optik*, **222** (2020), 165394. https://doi.org/10.1016/j.ijleo.2020.165394
13. M. Eslami, H. Rezazadeh, The first integral method for Wu-Zhang system with conformable time-fractional derivative, *Calcolo*, **53** (2016), 475–485. https://doi.org/10.1007/s10092-015-0158-8
14. M. Eslami, F. S. Khodadad, F. Nazari, H. Rezazadeh, The first integral method applied to the Bogoyavlenskii equations by means of conformable fractional derivative, *Opt. Quant. Electron.*, **49** (2017), 391. https://doi.org/10.1007/s11082-017-1224-z
15. I. Ullah, Dynamics behaviours of N-kink solitons in conformable Fisher-Kolmogorov-Petrovskii-Piskunov equation, *Eng. Computation.*, **2024** (2024), 358. https://doi.org/10.1108/ec-04-2024-0358
16. A. Gaber, H. Ahmad, Solitary wave solutions for space-time fractional coupled integrable dispersionless system via generalized kudryashov method, *Facta Univ.-Ser. Math.*, **35** (2020), 1439–1449. https://doi.org/10.22190/FUMI2005439G
17. Y. Pandir, Y. Gurefe, E. Misirli, The extended trial equation method for some time fractional differential equations, *Discrete Dyn. Nat. Soc.*, **2013** (2013), 491359. https://doi.org/10.1155/2013/491359
18. X. D. Zhang, Y. L. Feng, Z. Y. Luo, J. Liu, A spatial sixth-order numerical scheme for solving fractional partial differential equation, *Appl. Math. Lett.*, **159** (2025), 109265. https://doi.org/10.1016/j.aml.2024.109265
19. S. K. Sharma, D. Kumar, A numerical study of new fractional model for convective straight fin using fractional-order Legendre functions, *Chaos Soliton. Fract.*, **141** (2020), 110282. https://doi.org/10.1016/j.chaos.2020.110282
20. D. Kumar, K. Hosseini, F. Samadani, The sine-Gordon expansion method to look for the traveling wave solutions of the Tzitzéica type equations in nonlinear optics, *Optik*, **149** (2017), 439–446. https://doi.org/10.1016/j.ijleo.2017.09.066
21. I. Ullah, K. Shah, T. Abdeljawad, M. M. Alam, A. S. Hendy, S. Barak, Dynamics behaviours of kink solitons in conformable Kolmogorov-Petrovskii-Piskunov equation, *Qual. Theory Dyn. Syst.*, **23** (2024), 268. https://doi.org/10.1007/s12346-024-01119-4
22. O. Guner, A. Bekir, H. Bilgil, A note on exp-function method combined with complex transform method applied to fractional differential equations, *Adv. Nonlinear Anal.*, **4** (2015), 201–208. https://doi.org/10.1515/anona-2015-0019

23. I. Ullah, K. Shah, S. Barak, T. Abdeljawad, S. Barak, Pioneering the plethora of soliton for the (3+1)-dimensional fractional heisenberg ferromagnetic spin chain equation, *Phys. Scr.*, **99** (2024), 095229. https://doi.org/10.1088/1402-4896/ad6ae6

24. Y. K. Xie, Z. Wang, A ratio-dependent impulsive control of an SIQS epidemic model with non-linear incidence, *Appl. Math. Comput.*, **423** (2022), 127018. https://doi.org/10.1016/j.amc.2022.127018

25. Y. J. Jiang, J. T. Ma, High-order finite element methods for time-fractional partial differential equations, *J. Comput. Appl. Math.*, **235** (2011), 3285–3290. https://doi.org/10.1016/j.cam.2011.01.011

26. J. S. Duan, T. Chaolu, R. Rach, Solutions of the initial value problem for nonlinear fractional ordinary differential equations by the Rach-Adomian-Meyers modified decomposition method, *Appl. Math. Comput.*, **218** (2012), 8370–8392. https://doi.org/10.1016/j.amc.2012.01.063

27. R. Khalil, M. Al Horani, A. Yousef, M. Sababheh, A new definition of fractional derivative, *J. Comput. Appl. Math.*, **264** (2014), 65–70. https://doi.org/10.1016/j.cam.2014.01.002

28. R. Özarslan, Dünya bankası reel verileri İle gayri safi yurtiçi hasıla modeline conformable türev yaklaşımı, *Bilecik Şeyh Edebali Üniversitesi Fen Bilimleri Dergisi*, **7** (2020), 640361. https://doi.org/10.35193/bseufbd.640361

29. M. Bilal, J. Iqbal, R. Ali, F. A. Awwad, E. A. A. Ismail, Establishing breather and N-soliton solutions for conformable Klein-Gordon equation, *Open Phys.*, **22** (2024), 20240044. https://doi.org/10.1515/phys-2024-0044

30. L. Gelens, G. A. Anderson, J. E. Ferrell, Spatial trigger waves: positive feedback gets you a long way, *Mol. Biol. Cell*, **25** (2014), 3437–3716. https://doi.org/10.1091/mbc.e14-08-1306

31. M. Bilal, J. Iqbal, R. Ali, F. A. Awwad, E. A. A. Ismail, Exploring families of solitary wave solutions for the fractional coupled higgs system using modified extended direct algebraic method, *Fractal Fract.*, **7** (2023), 653. https://doi.org/10.3390/fractalfract7090653

32. B. Elma, E. Misirli, Two reliable techniques for solving conformable space-time fractional PHI-4 model arising in nuclear physics via β-derivative, *Rev. Mex. Fís.*, **67** (2021), 050707. https://doi.org/10.31349/RevMexFis.67.050707

33. I. Ullah, K. Shah, T. Abdeljawad, Study of traveling soliton and fronts phenomena in fractional Kolmogorov-Petrovskii-Piskunov equation, *Phys. Scr.*, **99** (2024), 055259. https://doi.org/10.1088/1402-4896/ad3c7e

34. M. Bilal, J. Iqbal, K. Shah, B. Abdalla, T. Abdeljawad, I. Ullah, Analytical solutions of the space-time fractional Kundu-Eckhaus equation by using modified extended direct algebraic method, *Partial Differential Equations in Applied Mathematics*, **11** (2024), 100832. https://doi.org/10.1016/j.padiff.2024.100832